

## Electronic Supplementary Information (ESI)

### Mesoporous Alloy Chiral Nanoparticles with High Production Yield and Strong Optical Activities

*Yicong Ma,<sup>a</sup> Lin Yang,<sup>b</sup> Yu Chen,<sup>c</sup> Xiaopeng Bai,<sup>d</sup> Geping Qu,<sup>e</sup> Tao Yao,<sup>f</sup> Xiangchen Hu,<sup>c</sup> Jianfang Wang,<sup>d</sup> Zongxiang Xu,<sup>e</sup> Yi Yu,<sup>c</sup> and Zhifeng Huang<sup>\*f</sup>*

<sup>a</sup>Department of Physics, Hong Kong Baptist University (HKBU), Kowloon Tong, Hong Kong SAR, China

<sup>b</sup>HKBU Institute for Research and Continuing Education Shenzhen, Guangdong 518057, China

<sup>c</sup>School of Physical Science and Technology, ShanghaiTech University, Shanghai, 201210, China

<sup>d</sup>Department of Physics, The Chinese University of Hong Kong, Shatin, NT, Hong Kong SAR, China

<sup>e</sup>Department of Chemistry, Southern University of Science and Technology, Shenzhen, Guangdong, 518055, China

<sup>f</sup>Department of Chemistry, The Chinese University of Hong Kong, Shatin, NT, Hong Kong SAR, China

E-mail: [zfhuang@cuhk.edu.hk](mailto:zfhuang@cuhk.edu.hk)

## Experimental Methods

### GLAD of the host Ag CNPs

The host CNPs were made of Ag. In a custom-built physical vapor deposition system (JunSun Tech Co. Ltd., Taiwan) with a high vacuum of  $10^{-7}$ - $10^{-6}$  Torr, metal pellets (Ag (99.999%), Fuzhou Innovation Photoelectric Technology Co., China) were evaporated at a rate of  $\approx 0.3$  nm  $s^{-1}$  as monitored by a quartz crystal microbalance (QCM) located near a substrate, using an electron-beam accelerating voltage of 8.0 kV, and emission current of 17–20 mA. At a deposition angle ( $a$ ) of  $86^\circ$  with respect to the normal direction of a substrate, Ag was evaporated on Si wafers (Semiconductor Wafer Inc., Taiwan) and sapphires (Meco Technology Ltd., Hong Kong) in an area of  $1.5 \times 1.5$  cm<sup>2</sup>. The substrate temperature was controlled at  $\approx -45$  °C, using an ethanol cooling system. To produce the RH- and LH-host with a given nominal helical pitch  $P$ , a substrate was rotated in clockwise and counterclockwise, respectively, at a rate  $R_r$  (in units of degree per second, or  $^\circ s^{-1}$ ) given by

$$R_r = 360 R_d / P_d \quad (S1)$$

where  $R_d$  is the deposition rate of Ag at the substrate surface calibrated as  $0.045$  nm  $s^{-1}$  at  $a$  of  $86^\circ$ , and  $P_d$  is the as-designed nominal  $P$ . The nominal  $P$  was experimentally evaluated by

$$P = H/m \quad (S2)$$

where  $H$  is the CNP height measured with scanning electron microscopy (SEM, Oxford, LEO 1530), and  $m$  is the number of substrate rotation during GLAD.

### Physical vapor deposition of Au adhesion layers

The Au adhesion layer was deposited with Au (99.999%, Fuzhou Innovation Photoelectric Technology Co., China) at  $a$  of  $0^\circ$  and  $R_d = 0.3$  nm  $s^{-1}$ , with an electron-beam accelerating voltage of 8.0 kV and emission current of 68–70 mA. The substrate was not rotated ( $R_r = 0$   $^\circ s^{-1}$ ), and the substrate temperature was controlled as  $\approx -45$  °C.  $T_{AL}$  was adjusted as a function of deposition duration.

### GLAD of the host $Ag_{1-x}Au_x$ CNPs

GLAD of the host binary  $Ag_{1-x}Au_x$  CNPs involved three sequential GLAD processes. The first and third step was the GLAD of the host Ag CNPs having a nominal  $P$  of roughly 8 nm and  $H$  of 40 nm. The second step was the deposition of dopant Au on the Ag CNPs, performed at  $a$  of  $86^\circ$ , substrate temperature of  $\approx -45$  °C,  $R_r = 0$   $^\circ s^{-1}$  (without substrate rotation) and  $R_d = 0.3$  nm  $s^{-1}$ , using an electron-beam accelerating voltage of 8.0 kV and emission current of 68–70

mA. The binary host was deposited on the adhesion layer of Au covering the supporting substrate.

### **GRR of the host**

In a homemade Teflon beaker, sapphire and silicon substrates deposited with the host were insert in a homemade Teflon holder and then immersed into a 200-mL electrolyte containing 20  $\mu\text{mol L}^{-1}$  chloroauric acid ( $\text{HAuCl}_4 \cdot 3\text{H}_2\text{O}$ , 99.999%, Sigma-Aldrich) at a stirring rate of 380 rpm under 25°C. Before the GRR, the Teflon holder and beaker were degreased in Piranha (98%  $\text{H}_2\text{SO}_4$ : 30%  $\text{H}_2\text{O}_2 = 3:1$ , v/v) for 15 min at room temperature, sufficiently rinsed with DI water (18.2 M $\Omega$ , Milli-Q reference water purification system fed with campus distilled water), and dried with  $\text{N}_2$  gases. After the GRR for 1–2 hr, the samples were removed out of the electrolyte to terminate the GRR and thoroughly rinsed with DI water and dried with  $\text{N}_2$  gases.

### **Optical Characterization**

Under ambient conditions, BioLogic CD (MOS 500) was used to monitor UV–visible–NIR extinction and CD spectra of a close-packed CNP array deposited on sapphire, under an irradiative incidence along the normal direction of sapphires. An extinction spectrum was monitored with an irradiation of linearly polarized light. For a given sample, four CD spectra in a wavelength range of 200–800 nm were subsequently recorded. After monitoring a CD spectrum, the sample was manually rotated at an angle of 90° around its normal axis before measuring the next CD spectrum. Then, the four CD spectra were algebraically averaged to obtain a CD spectrum of the sample, to eliminate linear birefringence and linear dichroism.

### **Structure Characterization**

The as-deposited samples were mechanically split, leaving the freshly exposed surfaces for the SEM-EDX (Carl Zeiss: LEO 1530) characterization. The CNPs were scratched off the substrates and well dispersed in water via ultrasonication for 30 min. Several drops of the mixture were applied to a TEM grid with lacey carbon film (Electron Microscopy Sciences, Inc., USA). The grid was dried under ambient conditions and characterized by TEM (Tecnai G2 20 STWIN). The High-resolution TEM, HAADF-STEM and EDS mapping were performed with a JEOL JEM-F200 field-emission gun microscope (200 kV, fitted with a JEOL silicon drift detector). Without post-deposition treatment, the samples were characterized by XRD (Bruker, non-monochromated Cu Ka X-ray with wavelength of 0.15418 nm, Advance

D8 multipurpose X-ray diffractometer) and XPS (ULVAC PHI 5000 VersaProbe III, Al Ka radiation of 1486.6 eV, at a current of 4.5 mA, voltage of 10 kV, and takeoff angle (between the sample and detector) of 45°, and in a vacuum of  $\approx 2 \times 10^{-9}$  mbar).

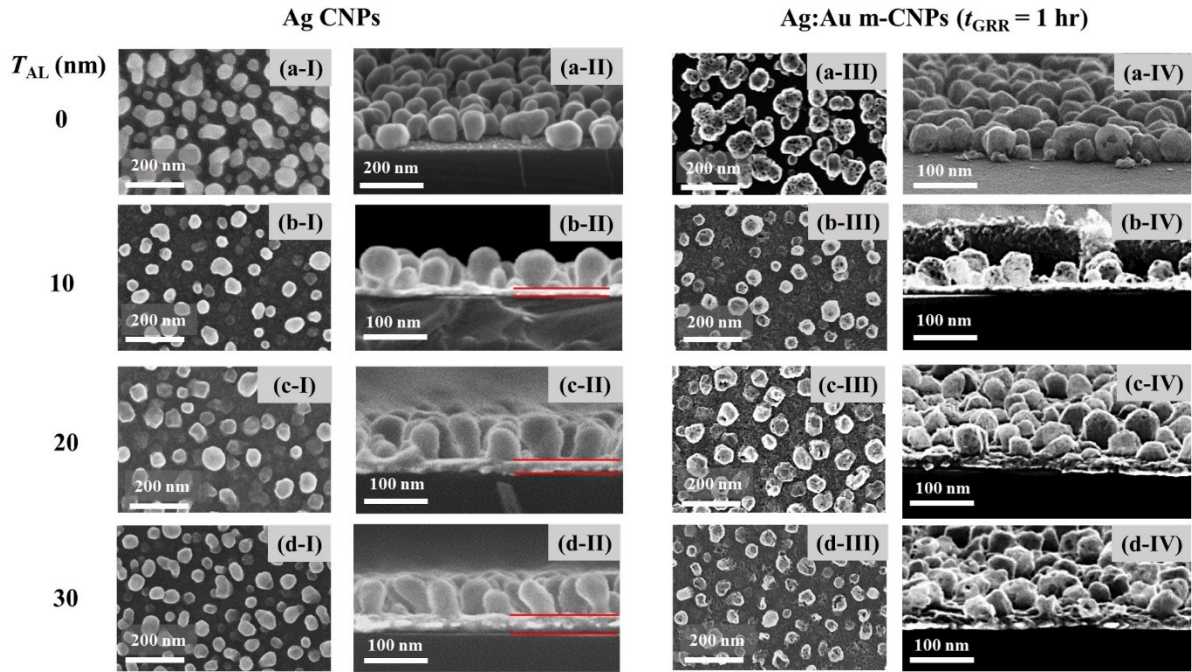


**Figure S1.** The GRR ( $t_{GRR}$  of 1 hr) of RH-Ag CNPs (with a nominal  $P$  of 8 nm and  $H$  of 80 nm) deposited on an Au adhesion layer with a  $T_{AL}$  of (a) 0 nm, (b) 10 nm, (c) 20 nm, and (d) 30 nm. (I, II) Ag CNPs; (III, IV) Ag:Au m-CNPs. (I, III) SEM top-down images; (II, IV) SEM cross-sectional images. (b-II, c-II, and d-II) The red lines show  $T_{AL}$ .

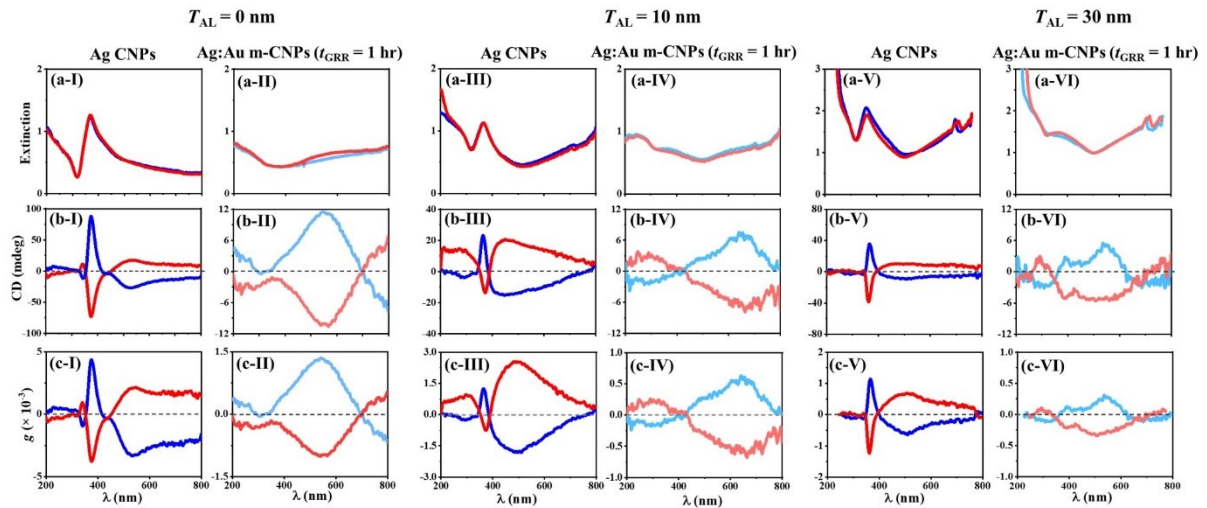


**Figure S2.** The 1 hr-GRR of Ag CNPs (with a nominal  $P$  of 8 nm and height  $H$  of 80 nm) deposited on an Au adhesion layer with a  $T_{AL}$  of (I, II) 0 nm, (III, IV) 10 nm, and (V, VI) 30 nm, characterized with the UV-visible-NIR spectroscopies of (a) extinction, (b) CD, and (c) anisotropic  $g$ -factor. (I, III, V) Ag CNPs; (II, IV, VI) Ag:Au m-CNPs produced with the 1-hr GRR. LH: red and pink lines; RH: blue and cyan lines.

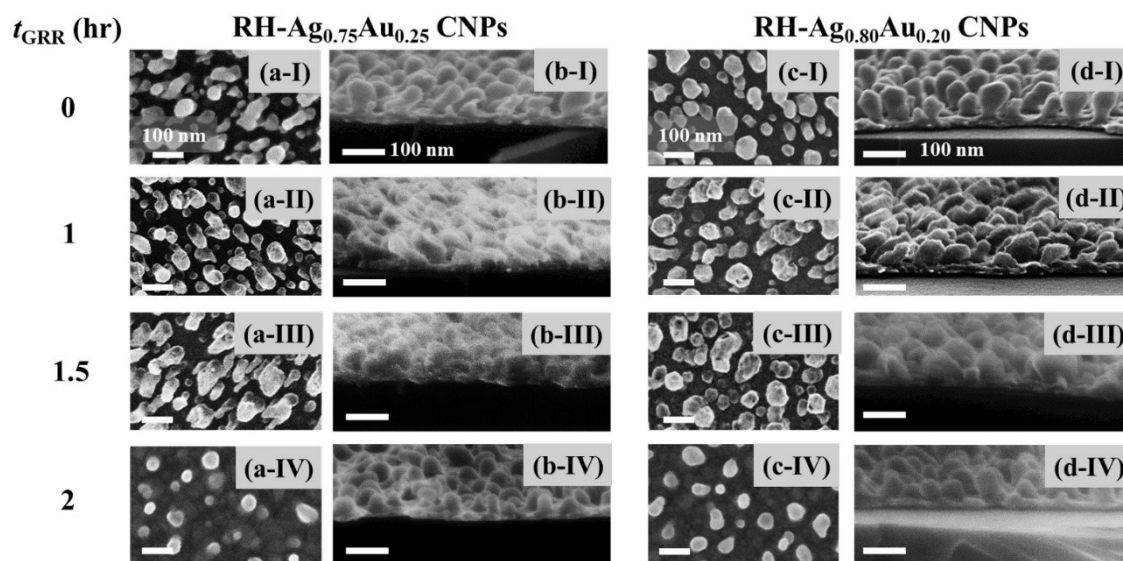


**Figure S3.** The GRR of (a, b) RH-Ag<sub>0.75</sub>Au<sub>0.25</sub> and (c, d) RH-Ag<sub>0.80</sub>Au<sub>0.20</sub> CNPs deposited on the Au adhesion layer (with  $T_{AL}$  of 20 nm), with the  $t_{GRR}$  of (I) 0, (II) 1, (III) 1.5 and (IV) 2 hr. SEM (a, c) top-down and (b, d) tilted images. Scale bars: 100 nm.

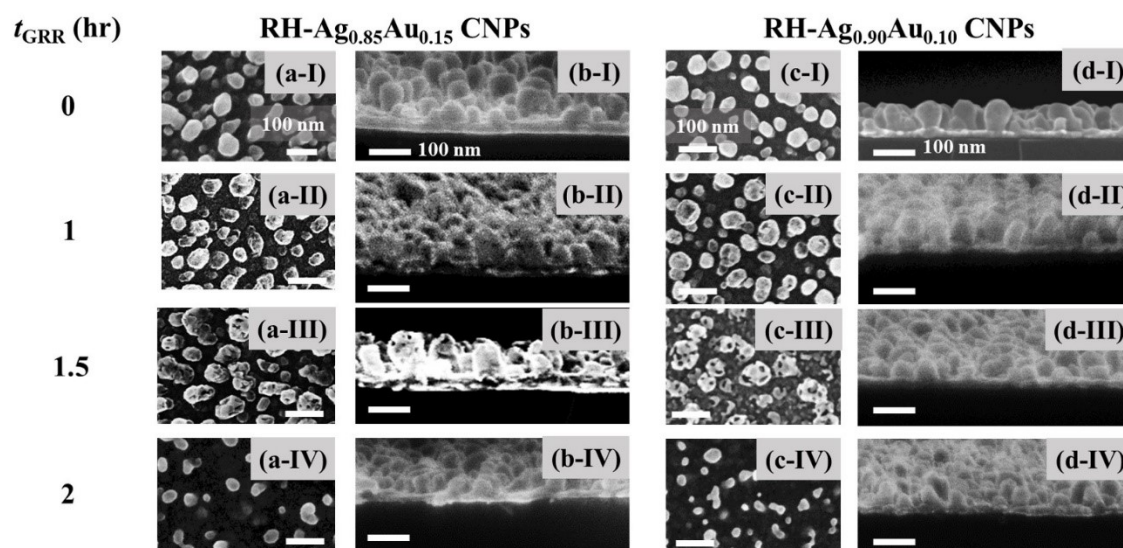


**Figure S4.** The GRR of (a, b) RH-Ag<sub>0.85</sub>Au<sub>0.15</sub> and (c, d) RH-Ag<sub>0.90</sub>Au<sub>0.10</sub> CNPs deposited on the Au adhesion layer (with  $T_{AL}$  of 20 nm), with the  $t_{GRR}$  of (I) 0, (II) 1, (III) 1.5 and (IV) 2 hr. SEM (a, c) top-down and (b, d) tilted images. Scale bars: 100 nm.

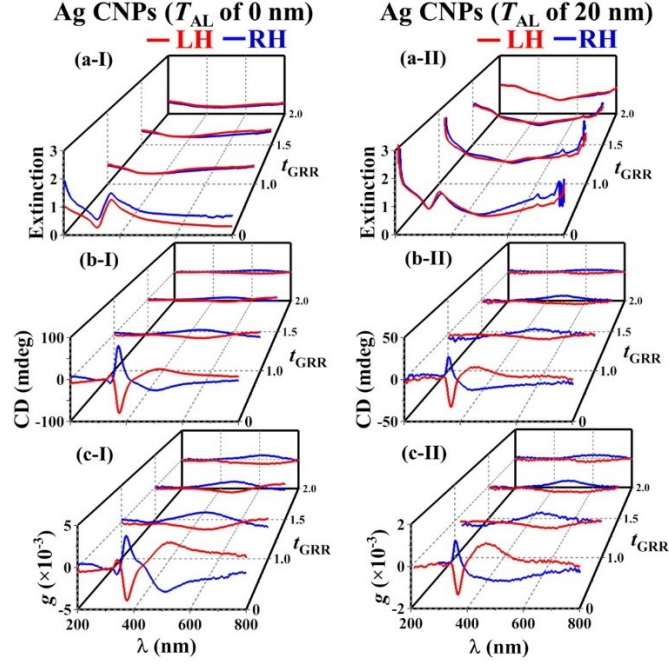


**Figure S5.** The GRR of Ag CNPs deposited on the Au adhesion layer with  $T_{AL}$  of (I) 0 nm and (II) 20 nm with the  $t_{GRR}$  increasing from 0 to 2 hr, characterized with UV-visible-NIR spectroscopies of (a) extinction, (b) CD, and (c) anisotropic  $g$ -factor. LH: red lines; RH: blue lines.

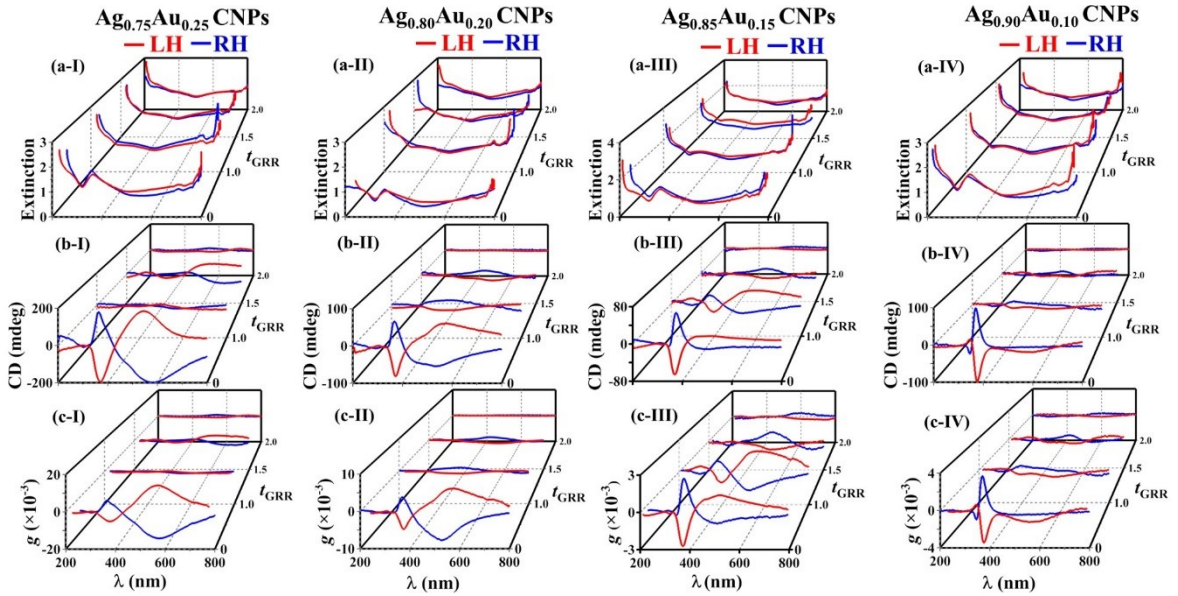


**Figure S6.** The GRR of (I)  $Ag_{0.75}Au_{0.25}$ , (II)  $Ag_{0.80}Au_{0.20}$ , (III)  $Ag_{0.85}Au_{0.15}$ , and (IV)  $Ag_{0.90}Au_{0.10}$  CNPs (deposited on the Au adhesion layer with the  $T_{AL}$  of 20 nm) with the  $t_{GRR}$  increasing from 0 to 2 hr, characterized with UV-visible-NIR spectroscopies of (a) extinction, (b) CD, and (c) anisotropic  $g$ -factor. LH: red lines; RH: blue lines.

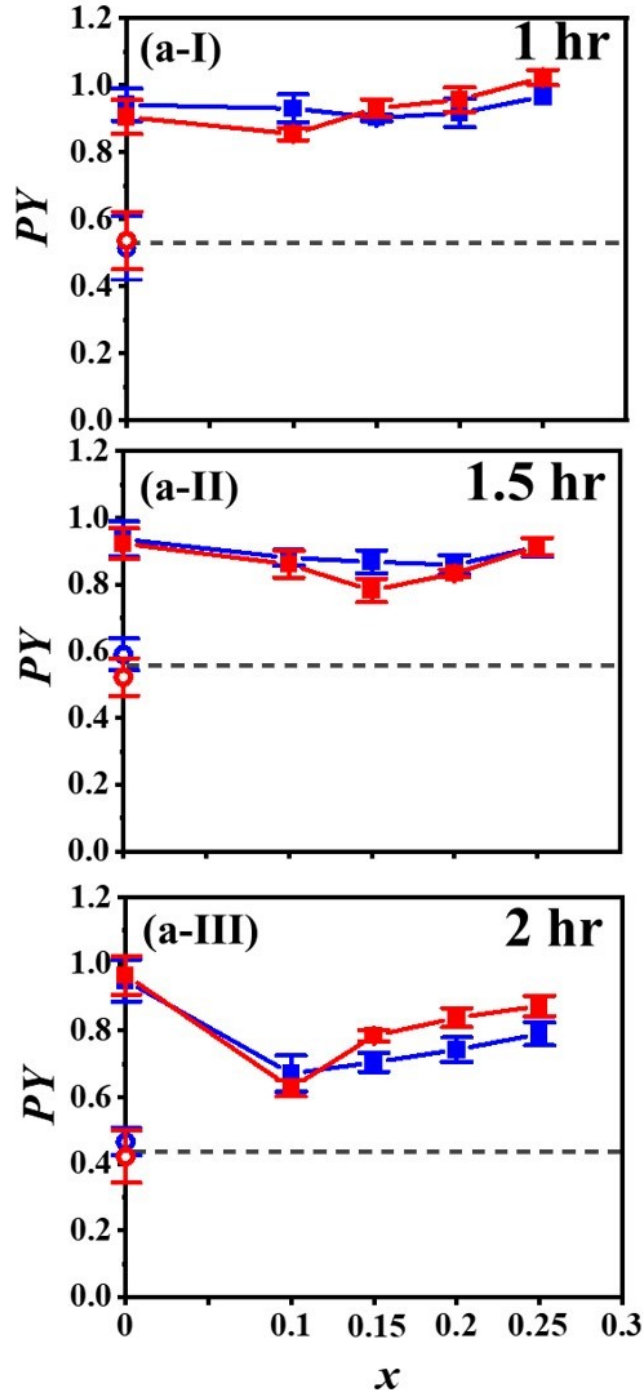


**Figure S7.** Plots of PY versus  $x$  for the GRR of binary  $\text{Ag}_{(1-x)}\text{Au}_x$  CNPs (deposited on the Au adhesion layer with the  $T_{\text{AL}}$  of 20 nm) with the  $t_{\text{GRR}}$  of (I) 1 hr, (II) 1.5 hr, and (III) 2 hr. LH: red solid squares; RH: blue solid squares. The results for the GRR of LH- and RH-Ag CNPs (without the Au adhesion layer) are shown with red and blue hollow spheres, respectively.



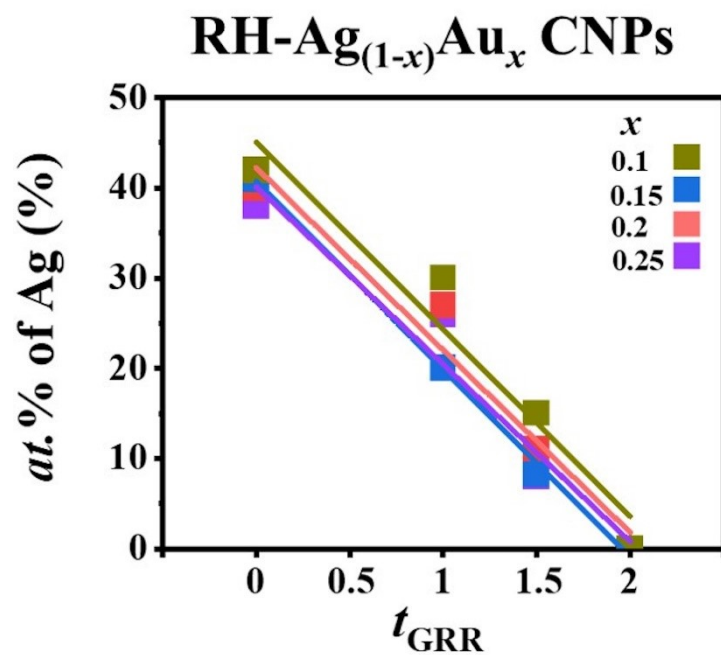


**Figure S8.** Plot of atomic percentage (at.%) of Ag in the RH-Ag:Ag m-CNPs versus  $t_{GRR}$ , for the GRR of RH-Ag<sub>(1-x)</sub>Au<sub>x</sub> CNPs deposited on the Au adhesion layer with the  $T_{AL}$  of 20 nm.  $x$  of 0.10 (Olive-green squares), 0.15 (blue squares), 0.20 (pink squares), and 0.25 (purple squares). The linear fitting leads to the evaluation of  $r_{GRR}$  as a function of  $x$ , as shown in **Figure 2c**.